

# Improved Haptic Transparency of Bilateral Control Using Torque-Measured Magnetic Coupling

Trieu-Khang Tu <sup>1</sup>, I-Haur Tsai <sup>2</sup>, Jia-Yush Yen <sup>2</sup>, Tsu-Chin Tsao <sup>3</sup> and Mi-Ching Tsai <sup>1,\*</sup>

<sup>1</sup> Department of Mechanical Engineering, National Cheng Kung University, Tainan 701401, Taiwan; n16077025@mail.ncku.edu.tw

<sup>2</sup> Department of Mechanical Engineering, National Taiwan University, Taipei 106319, Taiwan; d03522016@ntu.edu.tw (I.-H.T.); jyen@ntu.edu.tw (J.-Y.Y.)

<sup>3</sup> Department of Mechanical and Aerospace Engineering, University of California, Los Angeles, Los Angeles, CA 90095, USA; ttsao@g.ucla.edu

\* Correspondence: mctsai@mail.ncku.edu.tw; Tel.: +886-6-2757575 (ext. 62173)

**Abstract:** The integrity and transparency of a haptic feedback in a bilateral control is crucial for precise and accurate operators' sensation during human–machine interactions. Conventional master and slave bilateral control systems are often subject to unknown or unwanted disturbances and dynamics in the actuators and powertrain linkages that hamper the haptic feedback integrity and transparency. Force sensor torque sensing and feedback control are required to mitigate these effects. In contrast to the conventional approach of introducing torque sensing using a mechanical spring, this paper introduces a magnetic coupling as a torque sensor to detect reaction torque between the human input and the master actuator. Disturbance observer-based torque feedback control is designed to suppress the disturbances and tailor the haptic transparency dynamics. Experimental results on a virtual reality interaction system, which involves the steering wheel bilateral control in a cyber-physical driving simulator system, demonstrate the feasibility and effectiveness of the proposed method with improved haptic integrity and transparency.

**Keywords:** bilateral control; disturbance decoupling; haptic transparency; magnetic coupling; virtual reality



**Citation:** Tu, T.-K.; Tsai, I.-H.; Yen, J.-Y.; Tsao, T.-C.; Tsai, M.-C. Improved Haptic Transparency of Bilateral Control Using Torque-Measured Magnetic Coupling. *Machines* **2021**, *9*, 172. <https://doi.org/10.3390/machines9080172>

Academic Editor: José Machado

Received: 16 July 2021

Accepted: 16 August 2021

Published: 18 August 2021

**Publisher's Note:** MDPI stays neutral with regard to jurisdictional claims in published maps and institutional affiliations.



**Copyright:** © 2021 by the authors. Licensee MDPI, Basel, Switzerland. This article is an open access article distributed under the terms and conditions of the Creative Commons Attribution (CC BY) license (<https://creativecommons.org/licenses/by/4.0/>).

## 1. Introduction

The development of industrial applications using haptic feedback bilateral motion control is not only limited to purely physical human–machine interactions, but also includes virtual–cyber interactions in that visual, auditory, and tactile information can help to reinforce human operation. Visual and auditory information can be easily presented to the operator; however, it is difficult for the operator to feel the physical haptic feedback. Most of the human–machine interaction systems use vibration as the force/torque feedback, and not haptic feedback. It is known that haptic feedback can massively improve the experience of human–machine interaction, which is based on so-called bilateral motion control [1–3]. The bilateral control system design has been widely used in cyber-physical applications, such as surgery [4,5] and driving simulators [6–8].

For driving simulator application that integrates vehicle dynamic simulation software such as CarSIM, the bilateral control system that enables human–machine and virtual–cyber interaction is made up of the steering mechanism called the master, and the virtual steering platform called the virtual slave. The main feature of a bilateral control system is the synchronous motion control whereby the virtual steering wheel has the same motion as the master. With the addition of pedals, the motion of a virtual car can be fully controlled by a human operator. The schematic setup of the driving simulator is depicted in Figure 1 where the driving sensation of a real car, mimicked by the virtual car, is generated by CarSIM and transmitted to the master to reproduce a corresponding haptic feel.

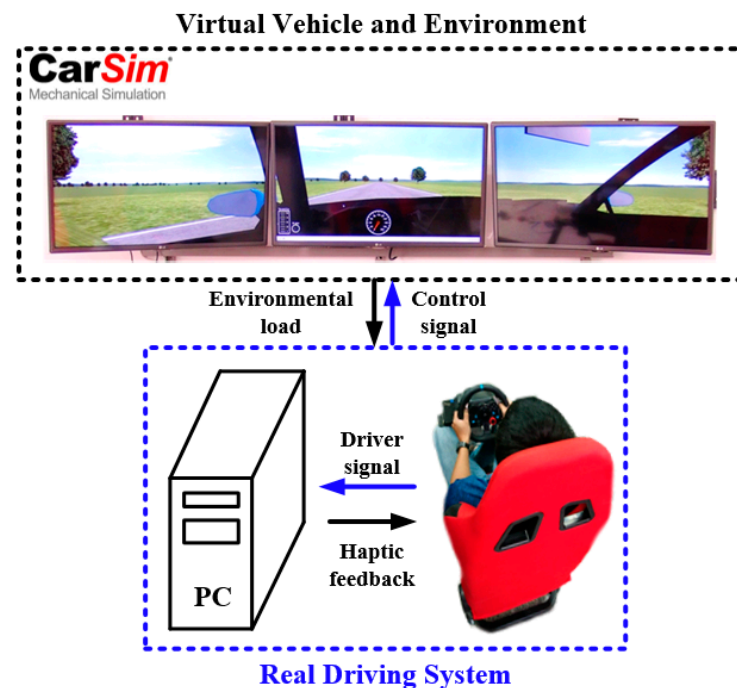


**Figure 1.** Schematic graph of the driving simulator system.

Based on the bilateral control scheme of [1], which directly utilizes the sum of external torques resulting from both master and slave sides and then feedforward to each control system, this study adopts the design of impedance control [9] for which an impedance model is proposed to specify the haptic feedback tailored for the required environment.

However, an identified problem that should be addressed, is the influence of other disturbances not caused by the environmental forces but present at the slave side. Since actual mechanisms such as steering systems are coupled to a driving motor, model inaccuracy and unwanted disturbances that are inherently present in the bilateral control system, will adversely influence the tactile sensation of the operator [10] and reduce the haptic transparency. These model inaccuracies and unwanted disturbances have been identified to emanate from the use of conventional torque sensors and mechanical coupling and links. Several solutions to improve haptic transparency performance have been presented, such as the use of torque sensors [11] or the observer control method [12,13]. The observer presented in [13] integrated a model-based disturbance compensation into the system to eliminate the negative effects of disturbances. The control performance of this method is highly dependent on the accuracy of an a priori known plant model.

Unlike the reviewed literature, this paper presents a different approach to bilateral control system, which combines the magnetic-coupler torque sensing with a disturbance observer for realizing haptic feedback. Moreover, the magnetic coupling as a component, does not only connect the steering wheel with the actuator, but also measures the relative position between the driver and driven sides. Unlike the commonly used mechanical flexible transmission mechanisms, such as torsion springs [14,15], magnetic coupling does not have any backlash [16,17], and its contactless characteristic can also provide inherent overload protection. As a result, the reaction torque responsible for reproducing haptic sensations to the operator can be detected and accurately measured by the magnetic coupling transmission module. Also, due to its frictionless and the elastic nature of its torsional stiffness, the magnetic coupling can provide a quick and smooth sensation of the reaction torque when operated within the admissible torque range. Furthermore, this paper presents an appropriate control scheme to deal with the disturbance feedforward compensation. The reaction torque measured from the magnetic coupling is used in the disturbance torque observer to decouple the load torque information. The model inaccuracy and external disturbances appearing on the driving motor installed in the master side can

be adequately observed and then compensated. The feasibility and effectiveness of the proposed method for improving haptic transparency in virtual reality applications were verified using a cyber-physical CarSIM driving simulator experimental system.

### 2. Bilateral Control Structure

As technology advances, bilateral control is being applied in many fields, such as surgery [18] and rehabilitation [19]. To realize a haptic feedback bilateral control system [20], the following two conditions should be satisfied:

$$\tau_m + \tau_v = 0, \tag{1}$$

$$\theta_m - \theta_v = 0, \tag{2}$$

where  $\tau$  and  $\theta$  denote the external torque and position of the motor, the subscripts  $m$  and  $v$  denote the master side and the virtual slave, respectively. Equation (1) shows that torque from each side needs to be balanced in the steady state. Then Equation (2) shows that for synchronization motion, the position control loops of both master and slave should follow the position command given by:

$$\theta^* = \frac{1}{2}(\theta_m + \theta_v). \tag{3}$$

The bilateral control [1] presented in this paper employed the feedforward control with specified reference model inertia. To provide the haptic feedback response setting, the impedance model approach employed at the speed-loop path is utilized as proposed in [21]. Figure 2 shows a bilateral motion control system, where  $K_t$ ,  $J$  and  $B$  are the motor parameters: torque constant, equivalent rotor inertia and damping respectively. Furthermore,  $K$  is the proportional gain of the position-loop controller,  $K_I$  and  $K_p$  denote the parameters of the speed-loop controller,  $C_\tau$  is the torque-loop feedforward gain, and  $J_{ref}$ ,  $B_{ref}$  are the parameters of a specified impedance model.

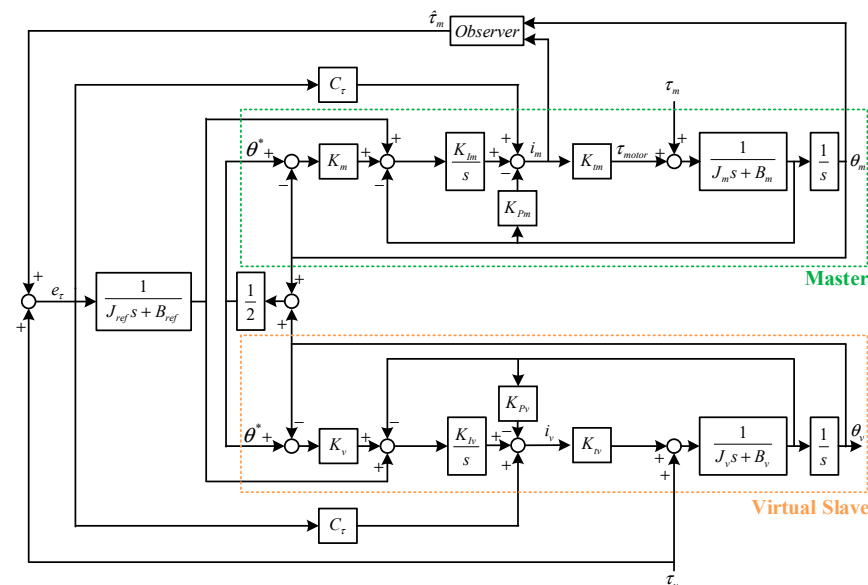


Figure 2. Torque observer-based bilateral control structure.

Synchronized motion control was presented in [22] which investigated the characteristics of the control structure. To understand the synchronous property of the bilateral control system depicted in Figure 2, let the feedforward reference model paths be removed as shown in Figure 3. Here,  $C_{vm}(s)$ ,  $C_{vv}(s)$  denote the velocity-loop controller, and the parameter  $\alpha \leq 1$  is regarded as the connecting bridge of the bilateral control system. Suppose

that the position gains are the same, consider  $K_m = K_v = K$  ( $K$  being the bandwidth of position loop), and that the bandwidth of the velocity loop is designed to be bigger than the position loop, then Figure 3 can be illustrated as Figure 4. When the input only comes from  $u_m$ , i.e., for the case of  $\tau_v = 0$  (i.e.,  $u_v = 0$ ), we can obtain:

$$\theta_m = \frac{s + (1 - \frac{\alpha}{2})K}{s^2 + 2(1 - \frac{\alpha}{2})Ks + (1 - \alpha)K^2} u_m, \tag{4}$$

$$\theta_v = \frac{\frac{\alpha}{2}K}{s^2 + 2(1 - \frac{\alpha}{2})Ks + (1 - \alpha)K^2} u_m. \tag{5}$$

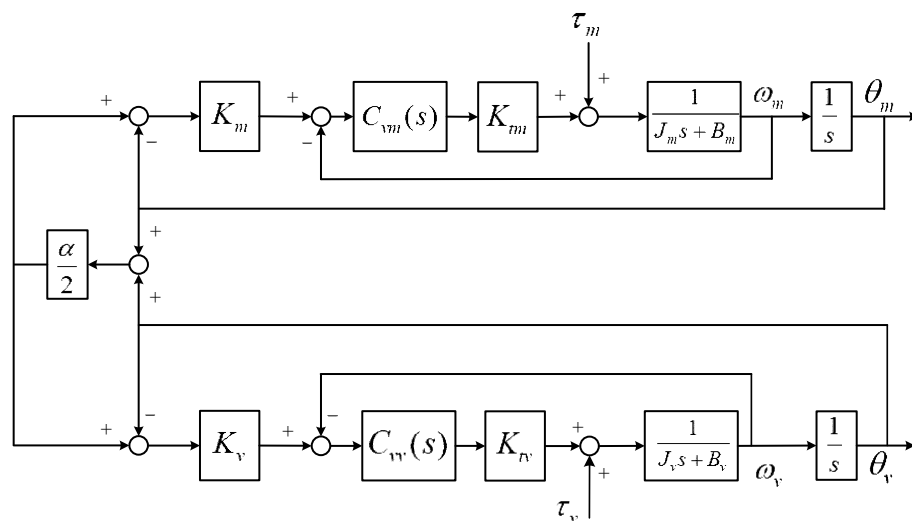


Figure 3. The internal position loop of bilateral control system.

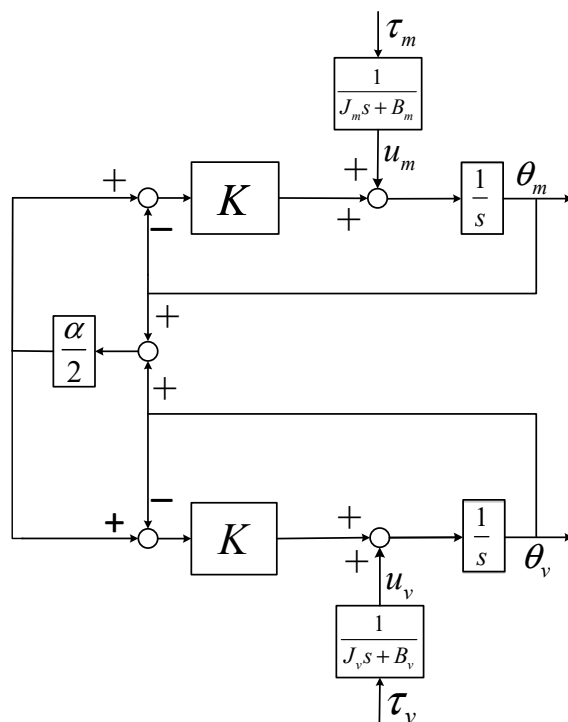


Figure 4. A simplified internal position loop of bilateral control system.

It can be found from Equations (4) and (5) that:

$$\frac{\theta_v}{\theta_m} = \frac{\frac{\alpha}{2}K}{s + (1 - \frac{\alpha}{2})K}. \tag{6}$$

As can be seen from Equations (4) and (5) for the case of  $\alpha = 1$ , the co-operated motion will be freely guided by the operator without difficulty. Obviously, when the torque input is from  $\tau_m$ ,  $\theta_v (\approx \theta_m)$  responds quickly. At the steady state, Equation (6) shows that  $\frac{\theta_v}{\theta_m} = \frac{\alpha}{2-\alpha} = 1$ . Conversely, when the torque input  $\tau_m$  is removed,  $\theta_v$  response terminates. The artificial viscous factor  $\alpha \leq 1$  can be employed to confirm the internal stability as needed.

### 3. Magnetic Coupling and Control Design Scheme

It is obvious that the effect of disturbances inherently appears when operating the steering mechanisms of the master side. The torque observer design can be employed to estimate the torque disturbance (i.e.,  $\tau_m + \tau_{dis}$ ) [23,24]. The observer for  $\hat{\tau}_m$  required in Figure 2 is shown in Figure 5 where  $K_{Po}$  and  $K_{Io}$  denote the parameters of the observer compensator, and “ $\hat{\phantom{x}}$ ” denotes a nominal model of the controlled plant and the related estimated information.

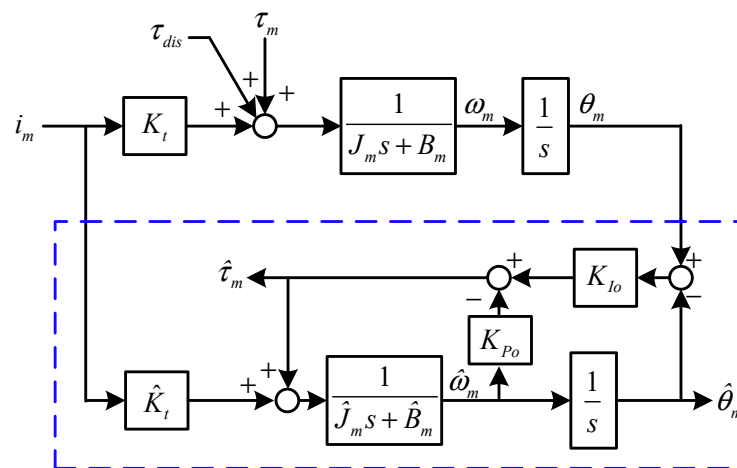


Figure 5. Disturbance observer.

From the torque disturbance observer shown in the blue dashed box of Figure 5, it can be found that for the case without modeling error,

$$J_m = \hat{J}_m, B_m = \hat{B}_m \text{ and } K_t = \hat{K}_t, \tag{7}$$

$$\frac{\hat{\tau}_m}{\tau_m + \tau_{dis}} = \frac{\frac{K_{Io}}{\hat{J}_m}}{s^2 + \frac{\hat{B}_m + K_{Po}}{\hat{J}_m}s + \frac{K_{Io}}{\hat{J}_m}}. \tag{8}$$

Obviously, the observed torque  $\hat{\tau}_m$  at the steady state will contain not only the unwanted disturbances  $\tau_{dis}$  such as uncertainties and parameter variation, but also the operator torque  $\tau_m$ , which reproduces haptic from external environmental load-torques applied to the slave. Since

$$\hat{\tau}_m \approx \tau_m + \tau_{dis}, \tag{9}$$

within the tailored dynamic bandwidth, the torque observer cannot distinguish the operator and the disturbance torque, the integrity and accuracy of the haptic sensation is compromised, where only the operator torque is wanted. Torque sensing has been employed [11] for improving haptic transparency performance. Torque measurements by relative displacement over a mechanical spring have been prevalent to the more-bulky and

costly strain gage-based torque sensors. We propose a torque-measured magnetic coupling approach with a modified configuration of the torque observer to suppress the disturbances and create reaction torque that follows the physical or virtual torque generated by the slave side. The magnetic coupling can be packaged as part of the motor drive and has an additional feature of limiting the level of the transmitted torque, which is important for human safety.

Magnetic coupling is a contactless and non-friction transmission mechanism that has a 1:1 gear ratio. Its contactless characteristic can be utilized in the steering system, such as [15] to provide transmission and smooth sensation compared to mechanical rigid contact couplings. The magnetic coupling also provides the function of overload protection for the situation while the motor driving torque is over the required safety. Because of the finite stiffness characteristic, the transmission torque of magnetic coupling can be easily measured by optical encoders as shown in Figure 6. A block diagram of the proposed transmission module for torque measurement is presented in Figure 7 where  $\tau_m$  denotes the operator torque, and  $\tau_{reac}$  denotes the reaction torque reproducing haptic to the operator where  $K_C$  is the stiffness constant of the coupling. As  $\hat{K}_C$  can be attained accurately using practical measurement, the coupling module is capable of detecting external reaction torque as follows:

$$\hat{\tau}_{reac} = \hat{K}_C(\theta_R - \theta_m). \quad (10)$$

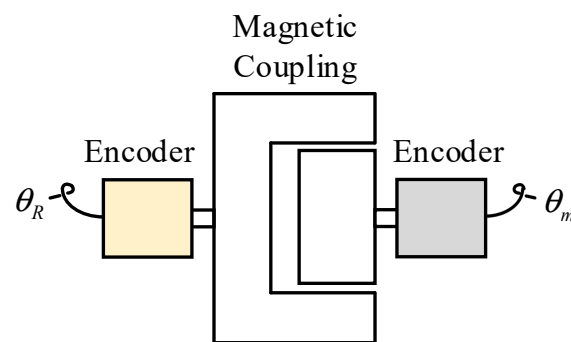


Figure 6. Schematic graph of magnetic coupling transmission module.

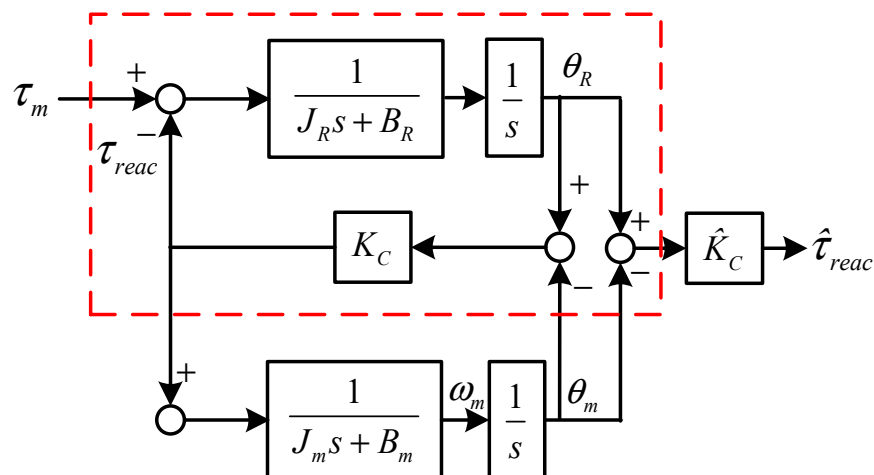


Figure 7. Block diagram of magnetic coupling transmission module.

Here, the magnetic coupling is employed to be a function as a torque sensor for measuring the external reaction torque  $\hat{\tau}_{reac}$  from its position difference. Unlike the rough sensation experience due to the high stiffness of torque sensors, the magnetic coupling can provide much smoother sensation and comfort for the operator when steering.

Based on the magnetic coupling of Figure 7, the overall structure of the bilateral motion control system with magnetic coupling is shown in Figure 8 where the dynamic

model of the magnetic coupling is represented by the Red dashed-line box. By using the estimated reaction torque, Equation (1) can be rewritten as:

$$\hat{\tau}_{reac} + \tau_v = 0. \tag{11}$$

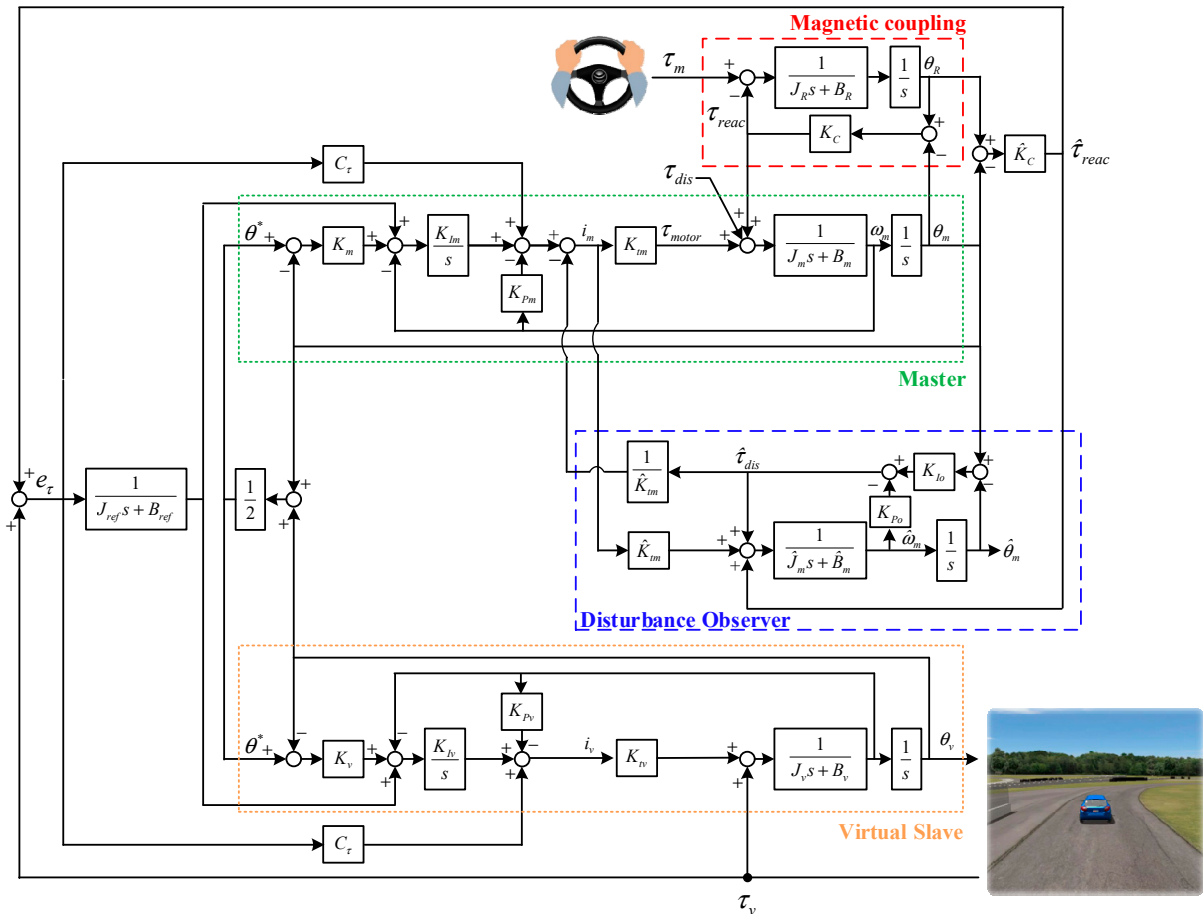


Figure 8. Block diagram of the proposed bilateral control configuration.

This implies that the reaction torque should be the same as environmental load torques applied to the slave in order to produce accurate haptic feedback. The remaining challenge is how to eliminate the effect of  $\tau_{dis}$ .

Since the virtual slave unit will not provide any physical disturbances and uncertainties, the control design that should be considered is only in the physical master unit. Figure 8 shows the overall configuration where the first layer sensor transmission module design is responsible for acquiring the reaction torque from the torque-measured magnetic coupling. Since the torque-measured magnetic coupling has no backlash,  $\hat{\tau}_{reac}$  can be obtained accurately by using high-resolution encoders. As can be seen, an internal loop disturbance feedforward compensation is proposed as shown in the blue dashed-line box in Figure 8 where the measured reaction torque  $\hat{\tau}_{reac}$  is utilized in the disturbance observer. By following the procedure of disturbance decoupling derivation given in [25], the transfer function from the disturbances  $\tau_{dis}$  to its observed  $\hat{\tau}_{dis}$  is the same as Equation (8). Suppose that the observer bandwidth is designed much larger than that of the speed control loop such that the transient response can be neglected, then

$$\hat{\tau}_{dis} \approx \tau_{dis}. \tag{12}$$

The modified disturbance observer with the measured reaction torque  $\hat{\tau}_{reac}$  can effectively estimate the unwanted disturbances  $\tau_{dis}$  which will then be eliminated as shown in

Figure 8. As the disturbances and/or parameter variation uncertainties can be decoupled properly by the feedforward compensation, the reaction torque measured by the magnetic coupling will only be induced from the virtual side (i.e.,  $\tau_{\text{reac}} \approx \hat{\tau}_{\text{reac}}$ ) in the bilateral control system. Thus, disturbance-free reaction torque is transmitted into the bilateral control system, which will be the same as the virtual load. As a result, the sensation of the haptic feedback felt by the operator can be effectively improved in the proposed bilateral control system.

#### 4. Experimental Results

To realize a cyber-physical car-driving simulator system, an experimental setup is shown in Figure 9a where a servomotor drive unit (400 W rated power output) is coupled with a high-resolution (i.e., 25,000 ppr designed also for use of the disturbance observer) encoder position sensor, a magnetic coupling, and a steering wheel that has an encoder on the master unit in order to develop a virtual steering system. On the slave unit, the CarSIM vehicle dynamic simulation tool is employed to establish the virtual car model and also the driving terrain. With the proposed bilateral control structure, an operator as shown in Figure 9b, which shows the experimental setup with a user performing the experiment, is able to drive the virtual car system by driving a steering wheel with an additional pedal unit. The virtual external load torque from the terrain's road conditions is generated by CarSIM according to the simulated vehicle speed and the terrain model, and then will transfer to the real-time Compact RIO Controller. The servomotor is controlled in real time to generate the physical torque sensation such that the operator's feel for the road conditions will be the same as a real driving experience. It should be noted that this approach is also useful for improving driver skills. The feasibility of the proposed cyber-physical car driving simulator system with haptic feedback is verified by the experimental results. To validate the improvement of the haptic feedback resulting from the proposed bilateral control, a comparison between using the conventional disturbance observer design depicted in Figure 2 and this proposed magnetic coupling design of Figure 8 were studied for performance evaluation. The designed bandwidth specifications of each motion loop, controller and model parameters for the control system depicted in Figure 8 are listed in Table 1.

**Table 1.** Parameters of system specifications.

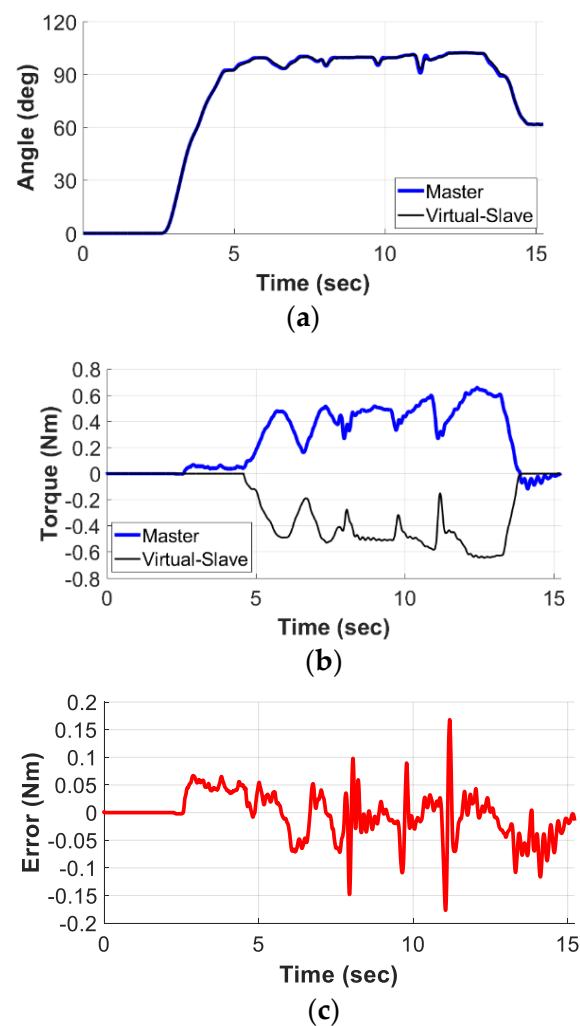
Symbol	Quantity	Value
$J_m, J_v$	Moment inertia	0.000226 kg·m <sup>2</sup>
$B_m, B_v$	Damping	0.00066 Nm·s/rad
$\hat{K}_C$	Estimated stiffness of coupling	6.25 Nm/rad
$\theta_m$	Resolution of encoder 1	25,000 ppr
$\theta_R$	Resolution of encoder 2	4096 ppr
$\omega_{oBW}$	Bandwidth of torque observer	100 Hz
$\omega_{vBW}$	Bandwidth of speed loop	20 Hz
$\omega_{pBW}$	Bandwidth of position loop	4 Hz
$K_{Io}$	Compensator gain of observer	215.4
$K_{Po}$	Compensator gain of observer	0.44
$K_{Im}, K_{Iv}$	speed controller gain of servomotor	17.66
$K_{Pm}, K_{Pv}$	speed controller gain of servomotor	0.18
$K_m, K_v$	position controller gain	25.13
$C_\tau$	Feedforward gain	3
$J_{ref}$	Moment inertia of reference model	0.0045 kg·m <sup>2</sup>
$B_{ref}$	Damping of reference model	0.0132 Nm·s/rad





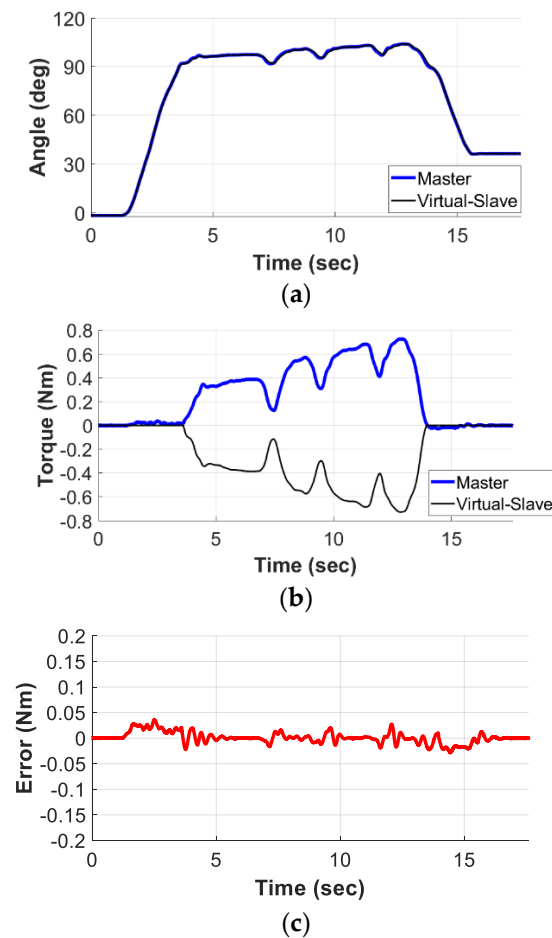
Figure 9. Picture of the (a) experimental setup, (b) user performing the experiment.

Figure 10 presents the results obtained from the torque observer bilateral control system of Figure 2 where Figure 10a shows the position responses of the physical steering system and the virtual plant of the steering wheel. As can be seen here, motion tracking performances between the two sides are in good agreement, which then has verified that the virtual car can be synchronously controlled by driving behavior. Figure 10b shows the measured haptic feedback torque and the virtual load from CarSIM and Figure 10c shows the torque error between these two torques ( $\tau_v$  and  $\tau_{reac}$ ). Obviously, the measured haptic feedback is observed not to be completely the same as the virtual load, when the virtual car is driving and contacting with the virtual terrain road. As depicted in Figure 10c, the maximum torque error is up to 0.15 Nm. This haptic performance reveals that the operator cannot completely feel the accurate external load torque due to the rough terrain. It should be noted that the virtual load simulated in the CarSIM was properly scaled to correspond with the actual experimental setup.



**Figure 10.** Results of conventional bilateral control: (a) position responses; (b) torque responses; (c) torque error.

By implementing the proposed bilateral control system of Figure 8, the experimental results are as shown in Figure 11. As can be seen, similar to Figure 10a, the results show a great position tracking performance. Moreover, the measured haptic feedback by the proposed disturbance compensation is also tracked very well and is consistent with the virtual load as measured by the magnetic coupling transmission module. It can be found from the results of Figures 10c and 11c that the torque error between  $\tau_v$  and  $\hat{\tau}_{reac}$  becomes much smaller (from 0.15 Nm to less than 0.05 Nm). This concludes that apart from the synchronous motion control between the real operator steering unit and the car moving simulation in the virtual reality system, as expected, the transparency of the haptic feedback can be effectively improved in the proposed bilateral control system.



**Figure 11.** Results of bilateral control using proposed magnetic coupling with the disturbance compensation method: (a) position responses; (b) torque responses; (c) torque error.

## 5. Conclusions

This paper has presented a bilateral control configuration using a torque-measured transmission module to improve tactile sensation. The haptic feedback was obtained without directly using a torque sensor, but with a magnetic coupling and position encoders attached, so that the observer configuration design and feedforward compensation structure can properly identify disturbances to ensure that the haptic feedback is only induced from the required virtual slave. The proposed control method was experimentally implemented in a cyber-physical car driving simulator system to verify the haptic performance. The experiment results suggest that the proposed control scheme is superior to that of the conventional bilateral control design in terms of the effect of both unwanted disturbances and haptic transparency. Future work includes making the master side more compact by integrating the servo-motor, position sensor and magnetic coupling as one unit, and conducting a usability analysis.

**Author Contributions:** Conceptualization, T.-C.T. and M.-C.T.; methodology, J.-Y.Y., T.-C.T. and M.-C.T.; validation, J.-Y.Y., T.-C.T. and M.-C.T.; formal analysis, T.-C.T. and M.-C.T.; investigation, T.-K.T. and I.-H.T.; writing—original draft preparation, T.-K.T. and I.-H.T.; writing—review and editing, J.-Y.Y., T.-C.T. and M.-C.T.; supervision, T.-C.T. and M.-C.T.; funding acquisition, M.-C.T. All authors have read and agreed to the published version of the manuscript.

**Funding:** This research was funded by Ministry of Science and Technology, Taiwan, under Grant No. 108-2917-I-002-024, 109-2918-I-006-001 and 109-2221-E-006-087-MY3.

**Institutional Review Board Statement:** Not applicable.

**Informed Consent Statement:** Not applicable.

**Data Availability Statement:** No new data were created or analyzed in this study. Data sharing is not applicable to this article.

**Conflicts of Interest:** The authors declare no conflict of interest.

## References

1. Katsura, S.; Matsumoto, Y.; Ohnishi, K. Realization of “Law of Action and Reaction” by Multilateral Control. *IEEE Trans. Ind. Electron.* **2005**, *52*, 1196–1205. [[CrossRef](#)]
2. Katsura, S.; Ohnishi, K. A realization of haptic training system by multilateral control. *IEEE Trans. Ind. Electron.* **2006**, *53*, 1935–1942. [[CrossRef](#)]
3. Motoi, N.; Kubo, R.; Shimono, T.; Ohnishi, K. Bilateral Control with Different Inertia Based on Modal Decomposition. In Proceedings of the IEEE International Workshop on Advanced Motion Control, Nagaoka, Japan, 21–24 March 2010; pp. 697–702.
4. Ogawa, K.; Ibrahim, M.Y.; Ohnishi, K. Development of Flexible Haptic Forceps Based on the Electrohydraulic Transmission System. *IEEE Trans. Ind. Inform.* **2018**, *14*, 5256–5267. [[CrossRef](#)]
5. Goh, H.; Kim, S.; Kang, S.G.; Lee, D.Y. Kinematic Requirements of a Haptic Interface for Simulation of Endonasal Endoscopic Skull Base Surgery. In Proceedings of the International Conference on Control, Automation and Systems, PyeongChang, Korea, 17–20 October 2018; pp. 39–44.
6. Yang, K.; Jie, J. The Designing of Training Simulation System Based on Unity 3D. In Proceedings of the International Conference on Intelligent Computation Technology and Automation, Shenzhen, China, 28–29 March 2011; pp. 976–978.
7. Ogitsu, T.; Mizoguchi, H. A study on driver training on advanced driver assistance systems by using a driving simulator. In Proceedings of the International Conference on Connected Vehicles and Expo, Shenzhen, China, 19–23 October 2015; pp. 352–353.
8. Lang, Y.; Wei, L.; Xu, F.; Zhao, Y.; Yu, L. Synthesizing Personalized Training Programs for Improving Driving Habits via Virtual Reality. In Proceedings of the Conference of IEEE Virtual Reality and 3D User Interfaces, Reutlingen, Germany, 18–22 March 2018; pp. 297–304.
9. Hogan, N. Impedance Control: An Approach to Manipulation: Part I—Theory, Part II—Implementation, Part III—Application. *J. Dyn. Syst. Meas. Control* **1985**, *107*, 1–23. [[CrossRef](#)]
10. Hangai, S.; Oda, K.; Nozaki, T.; Ohnishi, K. Fiber Suspended Micro Force Transmission System using Scaling Bilateral Control. In Proceedings of the Conference of IEEE Industrial Electronics Society, Washington, DC, USA, 21–23 October 2018; pp. 4575–4580.
11. Li, Y.F.; Chen, X.B. On the Dynamic Behavior of a Force/Torque Sensor for Robots. *IEEE Trans. Instrum. Meas.* **1998**, *47*, 304–308. [[CrossRef](#)]
12. Mizutani, Y.; Katsura, S. Micro-macro Bilateral Control with Compensation of Gravity and Friction. In Proceedings of the International Conference on Mechatronics, Vicenza, Italy, 27 February–1 March 2013; pp. 780–785.
13. Fukushima, S.; Sekiguchi, H.; Saito, Y.; Nozaki, T.; Ohnishi, K. Online Compensation of Gravity and Friction for Haptics with Incremental Position Sensors. In Proceedings of the International Conference on Mechatronics and Machine Vision in Practice (M2VIP), Auckland, New Zealand, 21–23 November 2017; pp. 1–6.
14. Lee, C.; Oh, S. Development, Analysis, and Control of Series Elastic Actuator—Driven Robot Leg. *Front. Neurobot.* **2019**, *13*, 17. [[CrossRef](#)] [[PubMed](#)]
15. Cheon, D.; Lee, C.; Oh, S.; Nam, K. Description of Steering Feel in Steer-By-Wire System Using Series Elastic Actuator. In Proceedings of the Conference of IEEE Vehicle Power and Propulsion, Hanoi, Vietnam, 14–17 October 2019; pp. 1–4.
16. Tlali, P.M.; Wang, R.; Gerber, S. Magnetic Gear Technologies: A Review. In Proceedings of the International Conference on Electrical Machines, Berlin, Germany, 2–5 September 2014; pp. 544–550.
17. Montague, R.G.; Bingham, C.M.; Atallah, K. Characterization and Modelling of Magnetic Couplings and Gears for Servo Control Systems. In Proceedings of the International Conference on Power Electronics, Machines and Drives, Brighton, UK, 19–21 April 2010; pp. 1–6.
18. Aoki, M.; Shimon, T.; Matsunaga, T.; Mizoguchi, T.; Shibao, S.; Sasaki, H.; Ohnishi, K. Identification Method of Environmental Stiffness Using Haptic Forceps for Brain Surgery. In Proceedings of the IEEE/ASME International Conference on Advanced Intelligent Mechatronics, Auckland, New Zealand, 9–12 July 2018; pp. 207–212.
19. Mitsantisuk, C.; Ohishi, K. Robotics-assisted Rehabilitation Therapy for the Hands and Wrists Using Force Sensorless Bilateral Control with Shadow and Mirror Mode. In Proceedings of the IEEE International Conference on Mechatronics (ICM), Nagoya, Japan, 6–8 March 2015; pp. 541–546.
20. Katsura, S.; Yamanouchi, W.; Yokokura, Y. Real-world Haptics: Reproduction of Human Motion. *IEEE Ind. Electron. Mag.* **2012**, *6*, 25–31. [[CrossRef](#)]
21. Hsueh, P.W.; Chen, J.C.; Yao, W.S.; Tsai, M.C.; Syu, W.C. Luenberger Observer-Based Impedance Control of Linear Servo Motor for a Desired Haptic System. In Proceedings of the International Conference on Automatic Control, Nantou, Taiwan, 2–4 December 2013; pp. 140–145.
22. Lorenz, R.D.; Schmidt, P.B. Synchronized Motion Control for Process Automation. In Proceedings of the IEEE Industry Applications Society Annual Meeting, San Diego, CA, USA, 1–5 October 1989; pp. 1693–1698.

- 
23. Yin, D.; Sun, N.; Hu, J.S. A Wheel Slip Control Approach Integrated with Electronic Stability Control for Decentralized Drive Electric Vehicles. *IEEE Trans. Ind. Inform.* **2019**, *15*, 2244–2252. [[CrossRef](#)]
  24. Hsueh, P.W.; Tsai, M.C. Reactive Torque Monitoring and Cycling Speed Control of a Belt-Driven Cycle Ergometer. *Control Eng. Pract.* **2013**, *21*, 1564–1576. [[CrossRef](#)]
  25. Ellis, G. *Observers in Control Systems: A Practical Guide*; Academic Press: San Diego, CA, USA, 2002.